GEM TN-92-97

Considerations on the Addition of Detector Planes Outside the GEM Magnet and on the Implementation of a Vertex Constraint

Larry Rosenson
Massachusetts Institute of Technology

April 9, 1992

Abstract:

An investigation has been made of the possible performance improvements of the muon system with the addition of a fourth superlayer and also with the inclusion of a vertex constraint. It is recommended that space be reserved for the addition of a detector layer outside the cryostat in the barrel region for a potential improvement in the resolution and increase in robustness/redundancy. The endcap resolution is found not to be subject to improvement with the addition of an extra layer. The vertex constraint is likely to yield significant improvement over the whole angular range and provision should be made to measure and maintain the required global alignment of the vertex detector to permit it's useful inclusion in the muon detector track reconstruction.

CONSIDERATIONS ON THE ADDITION OF DETECTOR PLANES OUTSIDE THE GEM MAGNET AND ON THE IMPLEMENTATION OF A VERTEX CONSTRAINT.

LARRY ROSENSON-MIT 4/9/92

ABSTRACT

An investigation has been made of the possible performance improvements of the muon system with the addition of a fourth superlayer and also with the inclusion of a vertex constraint. It is recommended that space be reserved for the addition of a detector layer outside the cryostat in the barrel region for a potential improvement in the resolution and increase in robustness/redundancy. The endcap resolution is found not to be subject to improvement with the addition of an extra layer. The vertex constraint is likely to yield significant improvement over the whole angular range and provision should be made to measure and maintain the required global alignment of the vertex detector to permit it's useful inclusion in the muon detector track reconstruction.

We have made a study of the improvement in performance and robustness to be expected from the addition of an additional superlayer external to the magnet and also by the inclusion of a vertex constraint in the determination of muon momentum from track measurements. The currently envisaged "baseline" magnet and muon system were used as a starting point for this investigation. The "baseline" system is of course a moving target and the details presented here may not be relevant for long , however the qualitative results and recommendations are expected to be valid for the GEM project.

Since the baseline GEM system is now being defined many structural decisions about the detector will be made in the near future which may preclude what would eventually be desirable changes and/or additions to the system. In this light we undertook a study of the potential performance gains to be garnered from:

1) The addition of an additional superlayer downstream of the minimal three superlayer array required for a stand alone muon system.

2) The inclusion of a vertex constraint in the determination of the muon momentum.

Both of the above additions to the minimal three point concept would carry with them some direct costs for hardware and, perhaps more importantly, require that care be taken during the definition of the system that their eventual inclusion not be blocked.

One might seek performance improvements of two very different kinds from any potential change to the muon system. The first is, of course, improvement of the momentum resolution. The open solenoid with forward

flux concentrator which we are in the process of adopting yields transverse momentum resolution about twice as good in the barrel region compared to the end cap region. It would be desirable to improve the forward resolution to approach more closely at least the currently anticipated performance of the barrel system. The second reason for undertaking a change or addition to the current system would be to make the system more robust in the sense of providing measurement redundancy. In particular, the vulnerability of the muon system to failure of the first superlayer by inundation with hadron and/or electromagnetic punch-through or other event associated background has always been a source of great concern. If this layer is swamped, because of unexpected high backgrounds at luminosity of $10^{33}/cm^2$ at startup or at the eventually anticipated $10^{34}/cm^2$, the three layer system currently envisaged would be useless. This nightmare scenario can be avoided if a backup measurement system is available either by the inclusion of a robust vertex constraint in the muon analysis or the inclusion of an additional superlayer at larger distances, or both. The safest backup might seem to be the external superlayer since direct measurement of a vertex point may be impossible due to a common mode failure of the tracker and muon system under high general or local rates. It may be argued that the vertex point will anyway be available through the spatial determination of the transverse beam position using tracks alone if the beam is stable enough. Obviously we will exploit this possibility if we can.

For reference, Fig. 1 shows the baseline transverse momentum (P_T) resolution. We note in passing that the resolution is significantly degraded for P_T less than ~ 100 GeV/c . This will be the case if Landau fluctuations of the energy loss are not recoverable calorimetricaly. In any event much of this degradation should be avoidable using the momentum measurement made in the central tracker.

For this study we assumed that the magnet coil and cryostat present 10 radiation lengths to a track passing through the coils and incident on an external barrel superlayer composed of two planes of detectors with the same precision and alignment properties as the internal barrel array.

In the end cap region we ignored the additional material that may be present in the flux concentrator support (the energies of interest here are higher than in the barrel region and the multiple scattering is correspondingly less important) and added a two plane superlayer with the same precision and alignment properties as the internal system downstream of each of the sections of the (split) internal system.

In Figs. 2-4 we show the ratio of the transverse momentum resolution with the external chambers to that of the baseline system, for several values of the separation of the external superlayer from the last internal superlayer.

In Fig 5, for the same configuration as in Fig. 2, we show the degradation of the resolution of the three plane system which results if the first plane is not

available and the external layer is. In the barrel region, for pseudorapidity(η) < 1, the resolution has been degraded by roughly a factor of two from the baseline performance for tracks with P_T above 1000 Gev/c. The low energy (< 500 Gev/c) resolution is seriously compromised over the whole barrel region. In this scenario the measurement available for $1 \leq \eta \leq 2$ is virtually useless , whereas the domain $2 \leq \eta \leq 2.5$ is marginally usable (e.g. sign determination will probably still be possible) . The reason for the poor performance of external planes at more forward angles is the field distortion caused by the flux concentrator and the general divergence of the magnetic field as it leaves the poleless magnet.

For the vertex constraint studies we include a vertex constraint as an additional measurement with a precision of either 100 μm or 200 μm. for the coordinate transverse to the beam and 6 cm/$\sqrt{12}$ for the longitudinal coordinate.

In Figs. 6 and 7 we show the improvement obtained over the baseline performance by the inclusion of the vertex constraint.

In Figs. 8 we show the combined effect of the vertex constraint and the external arrays for the case of Fig. 2 .

In Fig. 9 we show the resolution obtained if the first superlayer fails but the vertex is still available either as a direct measurement or through knowledge of the beam position. In the barrel region the resolution is limited by multiple scattering to about 10% at low P_T and, in fact, is <u>improved</u> with respect to the baseline above 1250 Gev/c . In the end cap region the situation is similar with the multiple scattering limit occurring at somewhat lower P_T.

In Fig. 10 we show the resolution obtained for the case of Fig. 2 if the first superlayer fails but the vertex and external array are available.

We would like to draw several conclusions from this information and to make several recommendations:

1-- The addition of the external chambers makes a significant contribution to the high energy resolution of the system mainly in the barrel region. In the small angle region the magnetic field shape at large distances is such that little gain in the resolution is achievable .
In the barrel region, up to about 35°, there is significant improvement above 500 GeV/c and this approach may be a cost effective way to improve the resolution.

We recommend that a region outside the magnet cryostat be left as clear of impediments as possible to permit the future inclusion of an external chamber array at least 3m. away from the third superlayer.

The alignment requirements for these external chambers is not as stringent as for the internal array by perhaps a factor of 2. The dependence of the resolution upon the radiation thickness of the coil is very weak because of the expected small number of radiation lengths in the coil/cryostat and the proximity of the coil to the additional superlayer (for some examples of this

situation and additional discussion see IMPROVEMENT OF MOMENTUM RESOLUTION USING MEASUREMENTS OUTSIDE THE MAGNET-LARRY ROSENSON-7/11/91-included in this GEM note as an Appendix).While the alignment specification is not so tight on the external array, the fact that there is no line of sight between inner and outer systems presents a conceptual and engineering challenge .It may, for example, be desirable to design tubes between the inner and outer cryostat walls, passing through the coil and cold region, to provide alignment sight paths.

One may be led by practical considerations to place the external chambers on the outside of the magnet cryostat container if it evolves into a thick enough annular cylinder.

2-- The inclusion of a vertex constraint in the analysis would result in an improvement across the whole angular region of 10%-30% above 1 TeV/c. It is probably worth implementing the vertex determination if at all possible since this is the only way we have thought of to improve the performance in the endcap region short of significantly increasing the total number of planes in the original 3 superlayers. The cost here will be largely in the development and implementation of a method of transferring the location of the vertex chamber to the reference frames of the main muon chamber array.

We recommend that conceptual and engineering studies of such an alignment system be undertaken as soon as possible to insure that competing design requirements do not preclude the eventual inclusion of the vertex constraint .

For completeness, in Fig. 11 we display the progressive improvement of the transverse momentum resolution if we successfully implement the above recommendations.

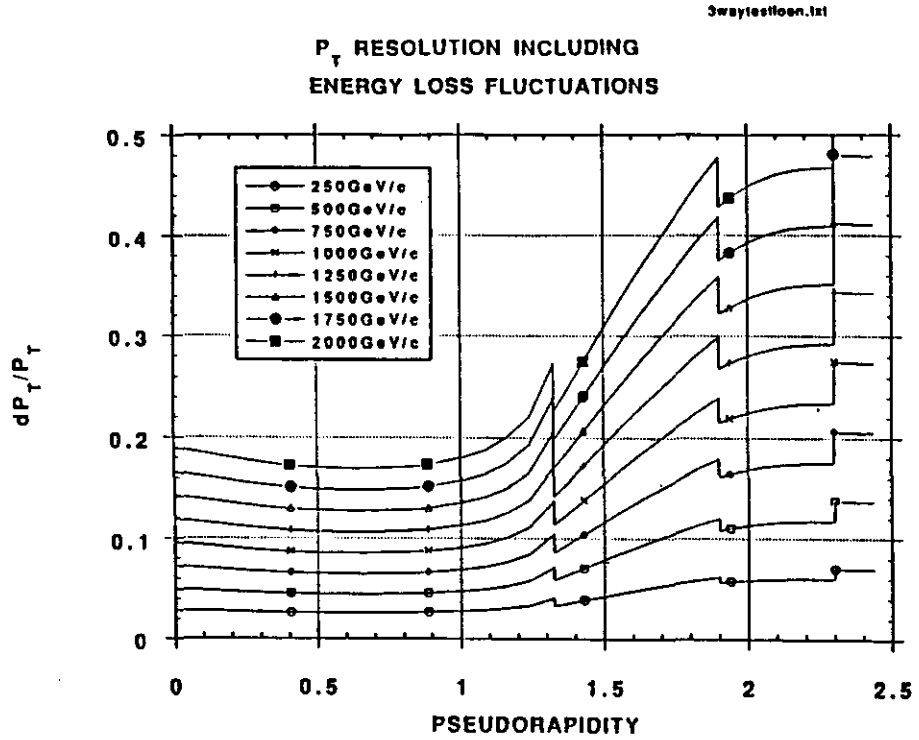
3wayteslloen.txt
P_T RESOLUTION INCLUDING
ENERGY LOSS FLUCTUATIONS
250GeV/c
500GeV/c
750GeV/c
1000GeV/c
1250GeV/c
1500GeV/c
1750GeV/c
2000GeV/c
dP_T/P_T
0.5
0.4
0.3
0.2
0.1
0
0
0.5
1
1.5
2
2.5
PSEUDORAPIDITY

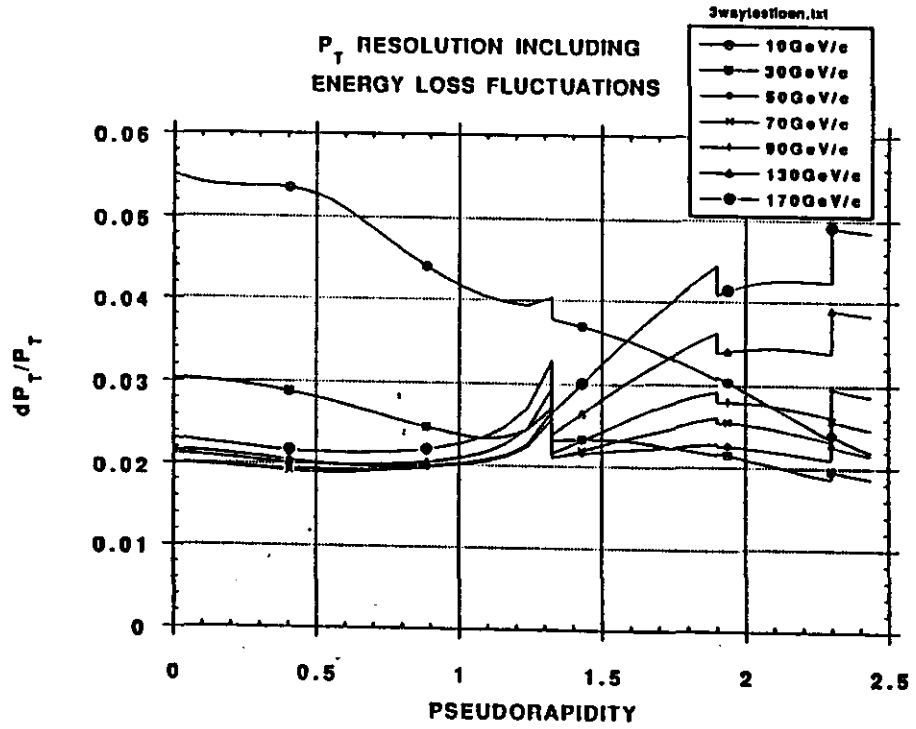
3wayteslloen.txt
P_T RESOLUTION INCLUDING
ENERGY LOSS FLUCTUATIONS
10GeV/c
30GeV/c
50GeV/c
70GeV/c
90GeV/c
130GeV/c
170GeV/c
dP_T/P_T
0.06
0.05
0.04
0.03
0.02
0.01
0
0
0.5
1
1.5
2
2.5
PSEUDORAPIDITY

Fig. 1

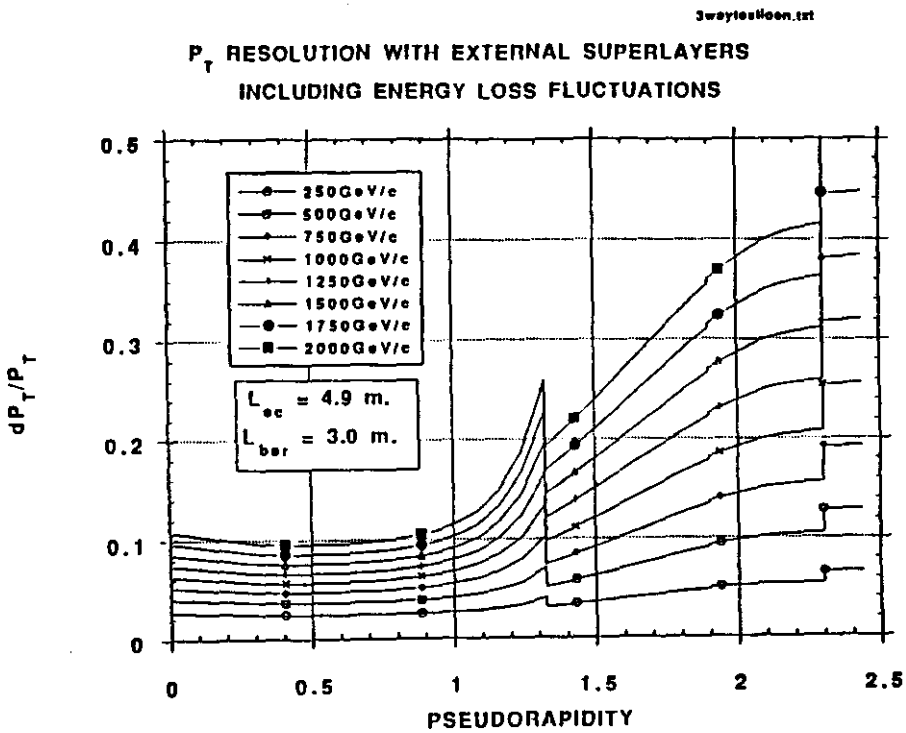
3waytestloon.txt
P_T RESOLUTION WITH EXTERNAL SUPERLAYERS
INCLUDING ENERGY LOSS FLUCTUATIONS
250GeV/c
500GeV/c
750GeV/c
1000GeV/c
1250GeV/c
1500GeV/c
1750GeV/c
2000GeV/c
L_ec = 4.9 m.
L_bar = 3.0 m.
dP_T/P_T
PSEUDORAPIDITY

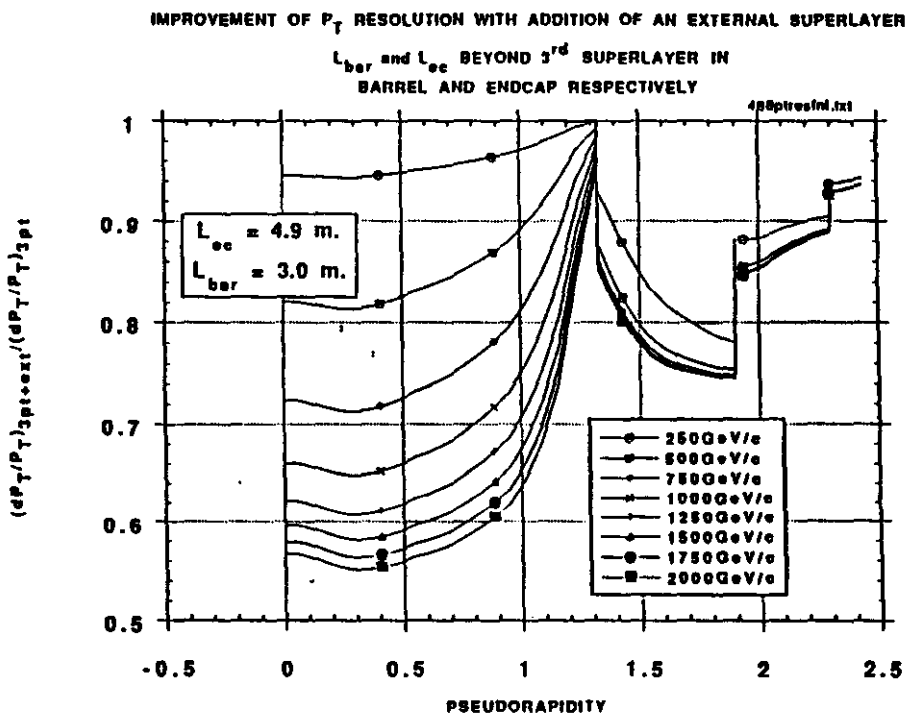
IMPROVEMENT OF P_T RESOLUTION WITH ADDITION OF AN EXTERNAL SUPERLAYER
L_bar and L_ec BEYOND 3rd SUPERLAYER IN
BARREL AND ENDCAP RESPECTIVELY
L_ec = 4.9 m.
L_bar = 3.0 m.
250GeV/c
500GeV/c
750GeV/c
1000GeV/c
1250GeV/c
1500GeV/c
1750GeV/c
2000GeV/c
(dP_T/P_T)_3pt+ext/(dP_T/P_T)_3pt
PSEUDORAPIDITY

Fig. 2

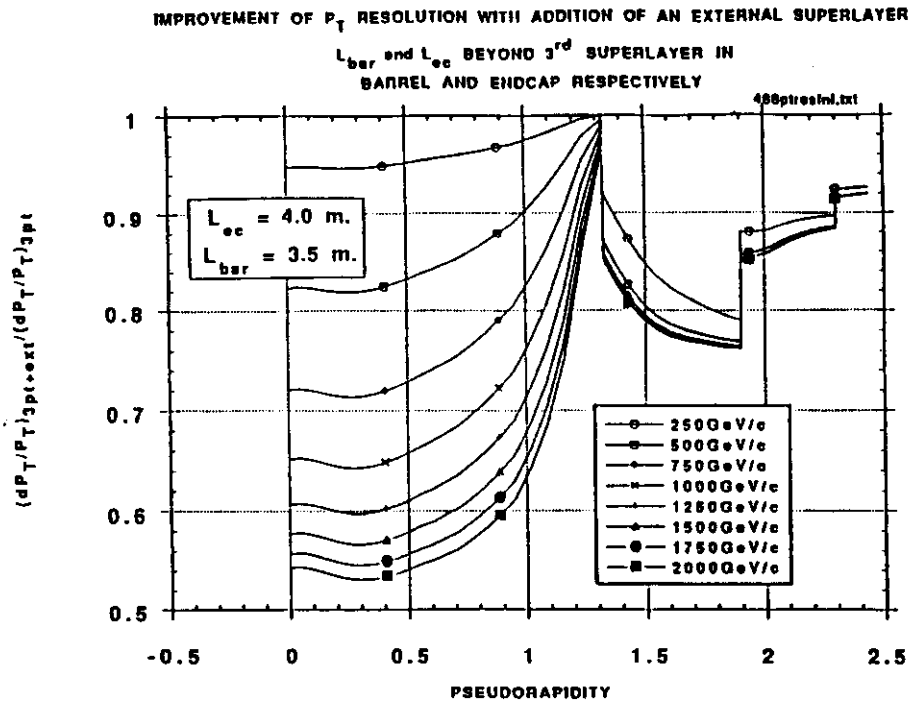
IMPROVEMENT OF P_T RESOLUTION WITH ADDITION OF AN EXTERNAL SUPERLAYER
L_{bar} and L_{ec} BEYOND 3rd SUPERLAYER IN
BARREL AND ENDCAP RESPECTIVELY
L_{ec} = 4.0 m.
L_{bar} = 3.5 m.
250GeV/c
500GeV/c
750GeV/c
1000GeV/c
1250GeV/c
1500GeV/c
1750GeV/c
2000GeV/c
$(dP_T/P_T)_{3pt+ext}/(dP_T/P_T)_{3pt}$
PSEUDORAPIDITY

Fig. 3

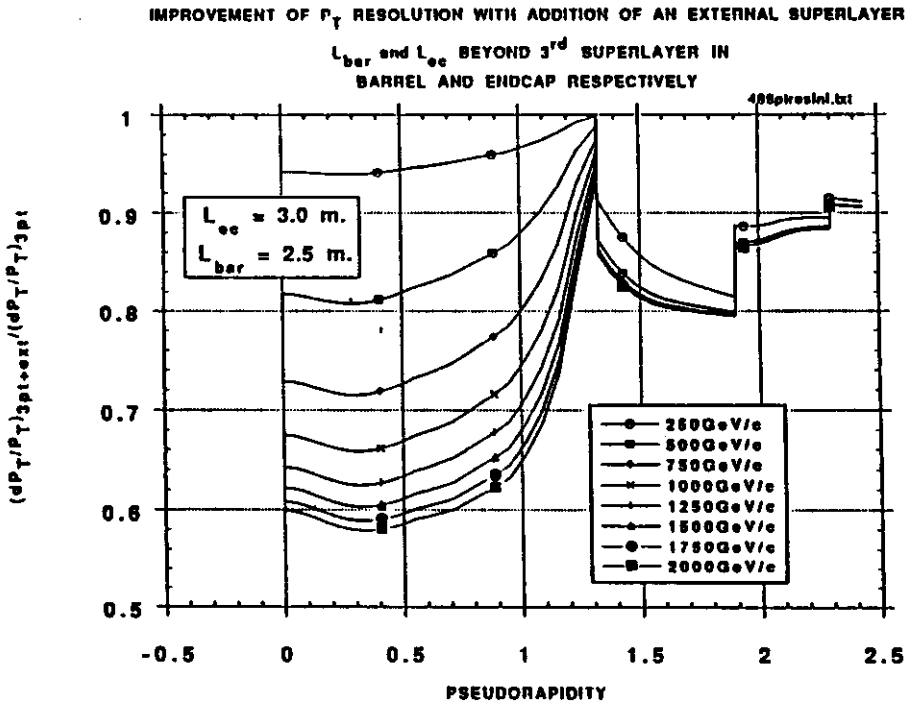
IMPROVEMENT OF P_T RESOLUTION WITH ADDITION OF AN EXTERNAL SUPERLAYER
L_{bar} and L_{ec} BEYOND 3rd SUPERLAYER IN
BARREL AND ENDCAP RESPECTIVELY
L_{ec} = 3.0 m.
L_{bar} = 2.5 m.
250GeV/c
500GeV/c
750GeV/c
1000GeV/c
1250GeV/c
1500GeV/c
1750GeV/c
2000GeV/c
$(dP_T/P_T)_{3pt+ext}/(dP_T/P_T)_{3pt}$
PSEUDORAPIDITY

Fig. 4

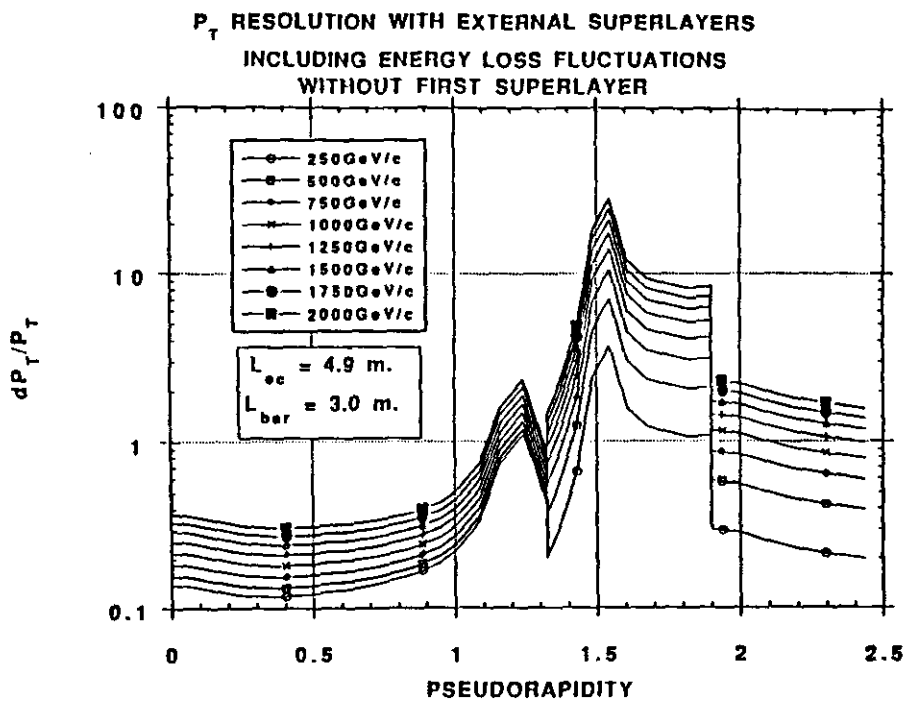
3waytestloen.txt
P_T RESOLUTION WITH EXTERNAL SUPERLAYERS
INCLUDING ENERGY LOSS FLUCTUATIONS
WITHOUT FIRST SUPERLAYER
250GeV/c
500GeV/c
750GeV/c
1000GeV/c
1250GeV/c
1500GeV/c
1750GeV/c
2000GeV/c
L_ec = 4.9 m.
L_bar = 3.0 m.
dP_T/P_T
100
10
1
0.1
0
0.5
1
1.5
2
2.5
PSEUDORAPIDITY

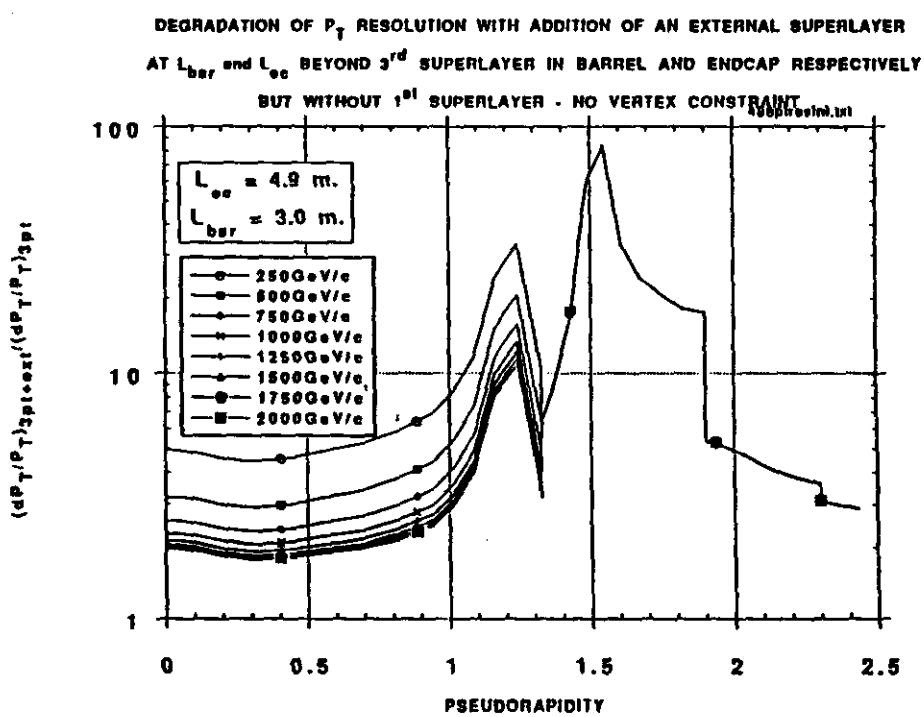
DEGRADATION OF P_T RESOLUTION WITH ADDITION OF AN EXTERNAL SUPERLAYER
AT L_bar and L_ec BEYOND 3rd SUPERLAYER IN BARREL AND ENDCAP RESPECTIVELY
BUT WITHOUT 1st SUPERLAYER - NO VERTEX CONSTRAINT
L_ec = 4.9 m.
L_bar = 3.0 m.
250GeV/c
500GeV/c
750GeV/c
1000GeV/c
1250GeV/c
1500GeV/c
1750GeV/c
2000GeV/c
(dP_T/P_T)3pt+ext/(dP_T/P_T)3pt
100
10
1
0
0.5
1
1.5
2
2.5
PSEUDORAPIDITY

Fig. 5

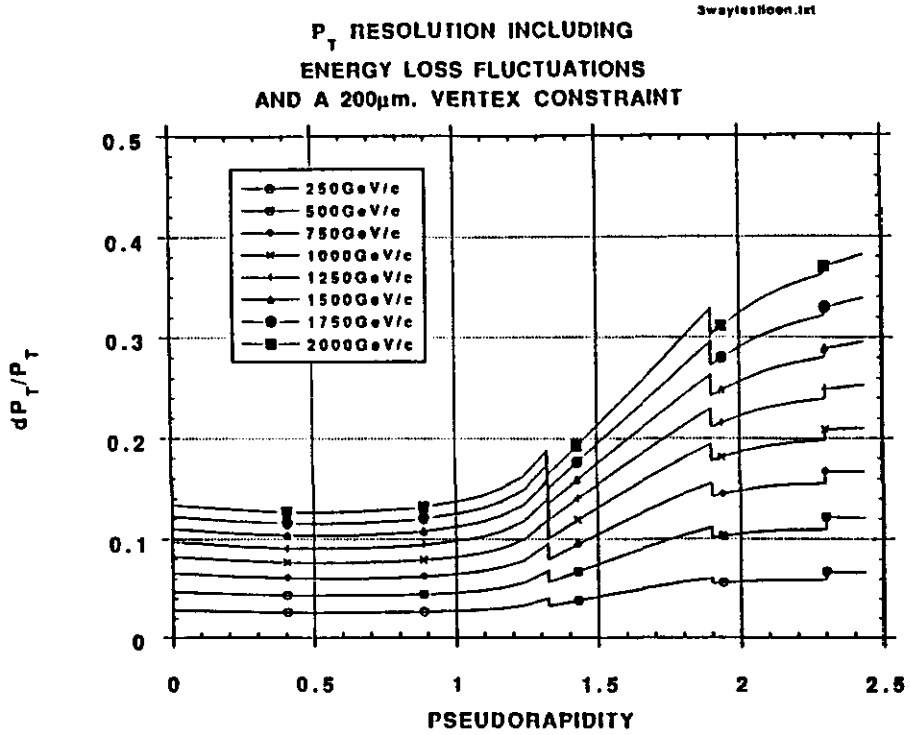
3waytestloon.txt
P_T RESOLUTION INCLUDING
ENERGY LOSS FLUCTUATIONS
AND A 200μm. VERTEX CONSTRAINT
250GeV/c
500GeV/c
750GeV/c
1000GeV/c
1250GeV/c
1500GeV/c
1750GeV/c
2000GeV/c
dP_T/P_T
0.5
0.4
0.3
0.2
0.1
0
0
0.5
1
1.5
2
2.5
PSEUDORAPIDITY

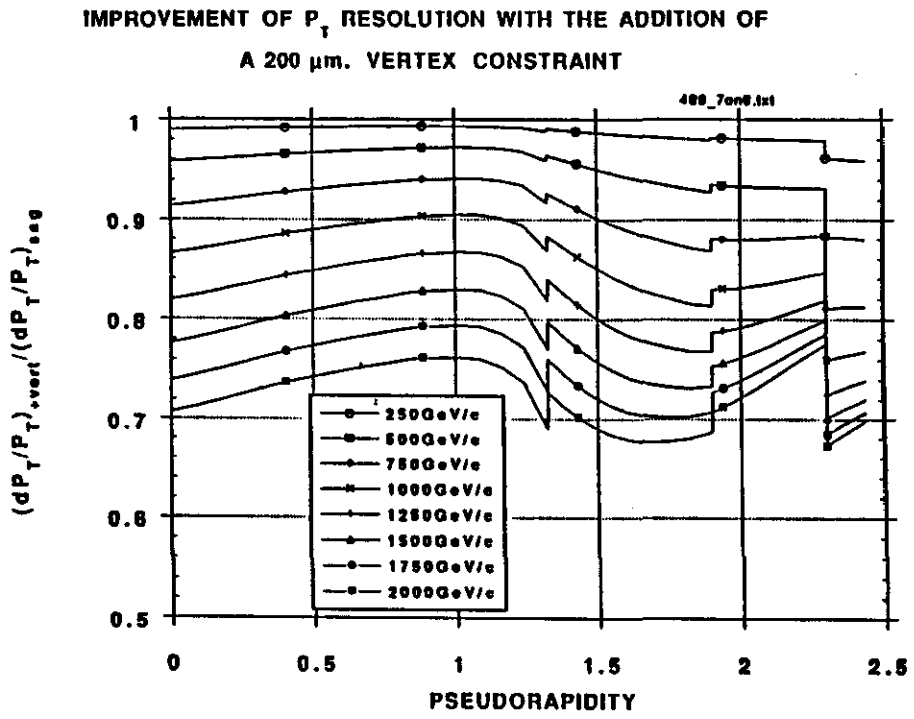
IMPROVEMENT OF P_T RESOLUTION WITH THE ADDITION OF
A 200 μm. VERTEX CONSTRAINT
$(dP_T/P_T)_{+vert}/(dP_T/P_T)_{seg}$
1
0.9
0.8
0.7
0.6
0.5
250GeV/c
500GeV/c
750GeV/c
1000GeV/c
1250GeV/c
1500GeV/c
1750GeV/c
2000GeV/c
0
0.5
1
1.5
2
2.5
PSEUDORAPIDITY

Fig. 6

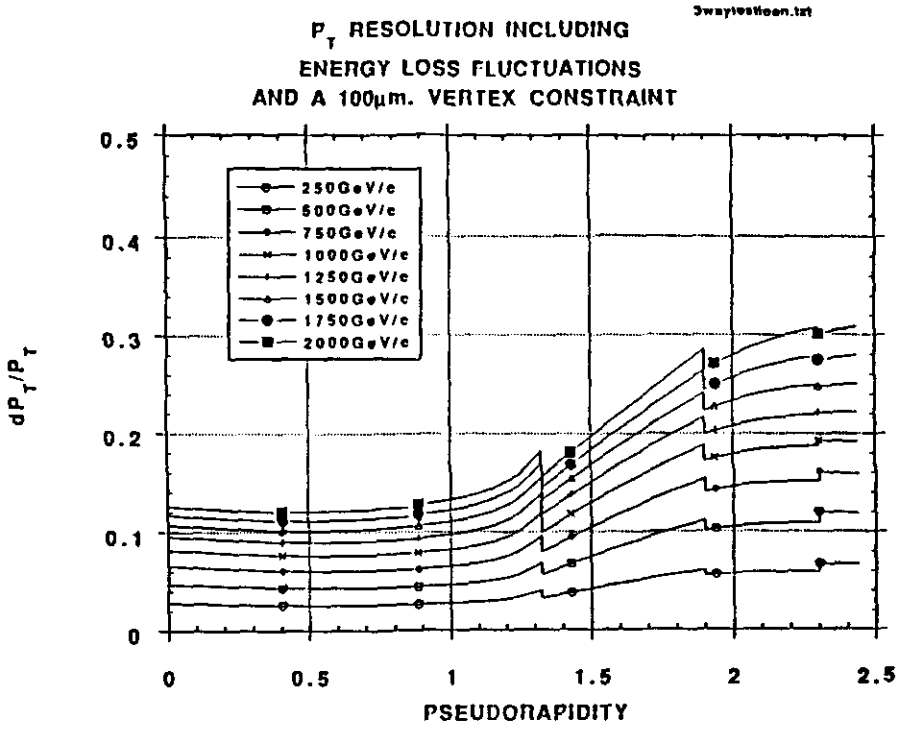
3waytestloon.txt
P_T RESOLUTION INCLUDING
ENERGY LOSS FLUCTUATIONS
AND A 100μm. VERTEX CONSTRAINT
250GeV/c
500GeV/c
750GeV/c
1000GeV/c
1250GeV/c
1500GeV/c
1750GeV/c
2000GeV/c
dP_T/P_T
0.5
0.4
0.3
0.2
0.1
0
0
0.5
1
1.5
2
2.5
PSEUDORAPIDITY

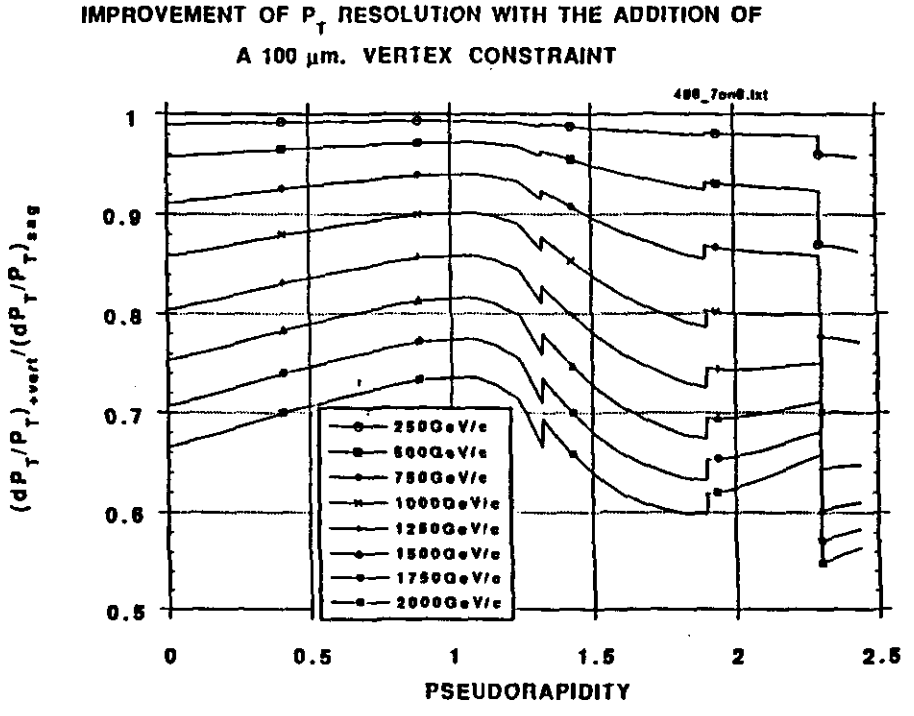
IMPROVEMENT OF P_T RESOLUTION WITH THE ADDITION OF
A 100 μm. VERTEX CONSTRAINT
$(dP_T/P_T)_{+vert}/(dP_T/P_T)_{sag}$
1
0.9
0.8
0.7
0.6
0.5
250GeV/c
500GeV/c
750GeV/c
1000GeV/c
1250GeV/c
1500GeV/c
1750GeV/c
2000GeV/c
0
0.5
1
1.5
2
2.5
PSEUDORAPIDITY

Fig. 7

GEM P_T RESOLUTION 3 POINT MEASUREMENT + EXTERNAL SUPERLAYER

3 m. AND 4.9 m. DOWNSTREAM OF 3rd SUPERLAYER
IN BARREL AND ENDCAP RESPECTIVELY
+ 200 μm. VERTEX CONSTRAINT

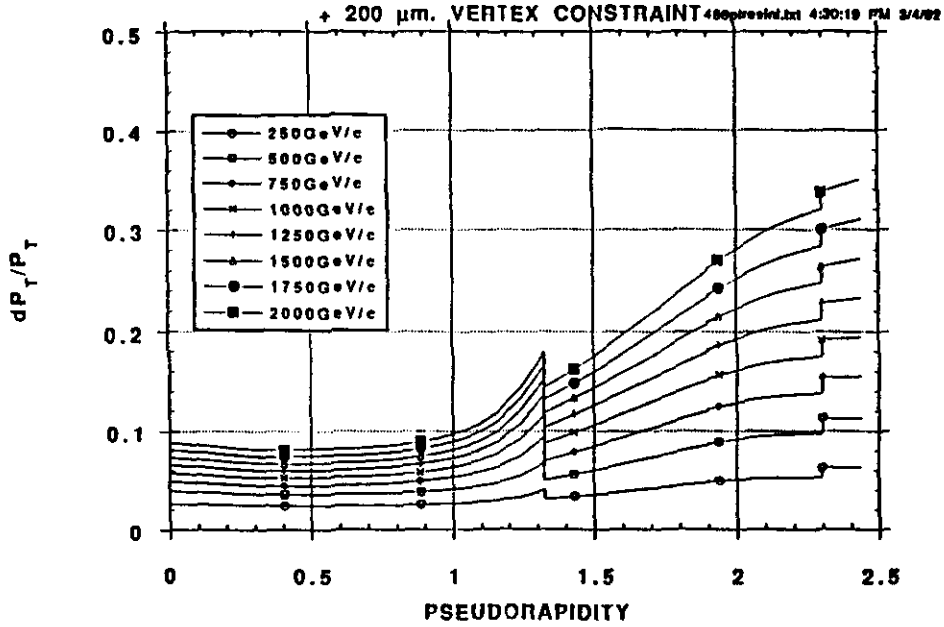

IMPROVEMENT OF P_T RESOLUTION WITH ADDITION OF AN EXTERNAL SUPERLAYER

3 m. AND 4.9 m. BEYOND 3rd SUPERLAYER IN BARREL AND ENDCAP RESPECTIVELY
+ A 200 μm. VERTEX CONSTRAINT

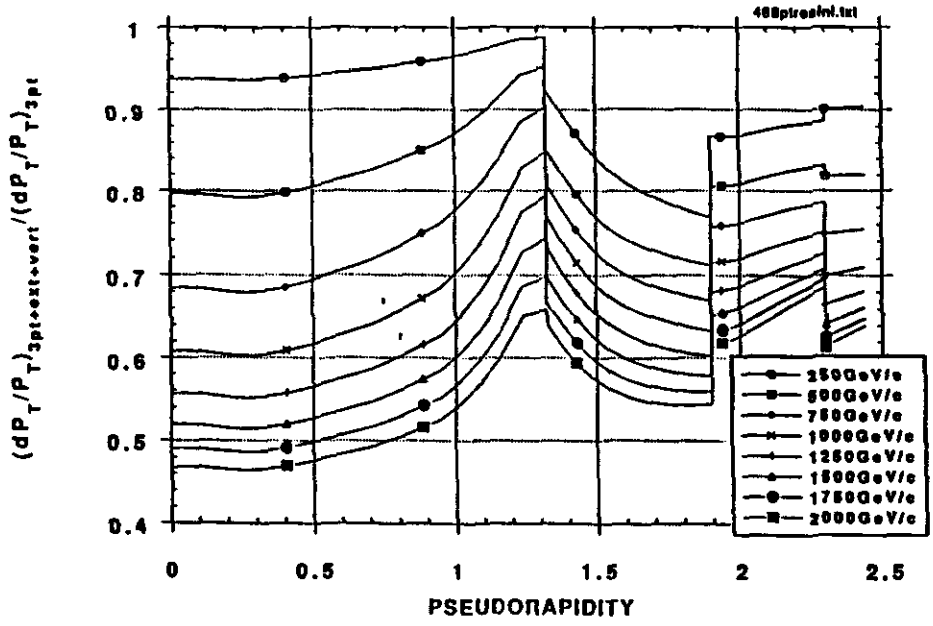

Fig. 8

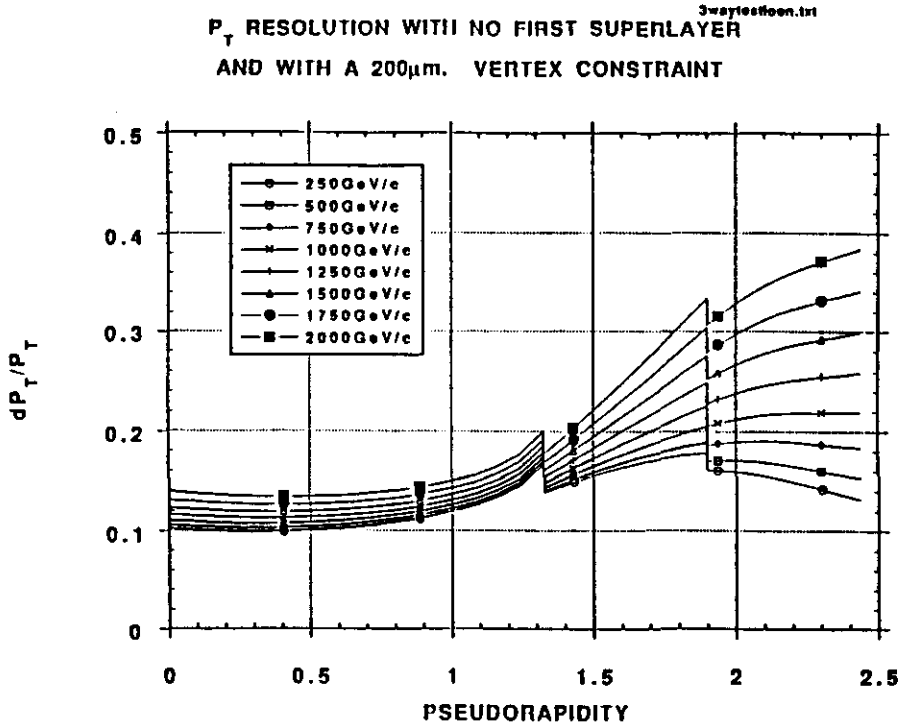
3waytestlcen.txt
P_T RESOLUTION WITH NO FIRST SUPERLAYER
AND WITH A 200μm. VERTEX CONSTRAINT
250GeV/c
500GeV/c
750GeV/c
1000GeV/c
1250GeV/c
1500GeV/c
1750GeV/c
2000GeV/c
dP_T/P_T
0.5
0.4
0.3
0.2
0.1
0
0
0.5
1
1.5
2
2.5
PSEUDORAPIDITY

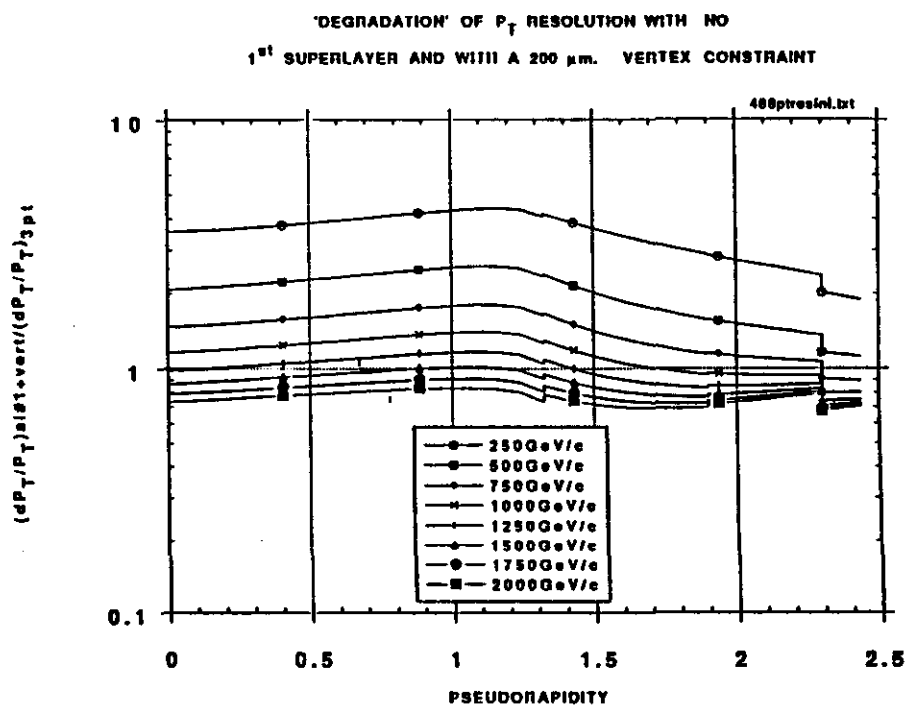
'DEGRADATION' OF P_T RESOLUTION WITH NO
1st SUPERLAYER AND WITH A 200 μm. VERTEX CONSTRAINT
488ptresini.txt
(dP_T/P_T)al#1+vert/$(dP_T/P_T)_{3pt}$
10
1
0.1
250GeV/c
500GeV/c
750GeV/c
1000GeV/c
1250GeV/c
1500GeV/c
1750GeV/c
2000GeV/c
0
0.5
1
1.5
2
2.5
PSEUDORAPIDITY

Fig. 9

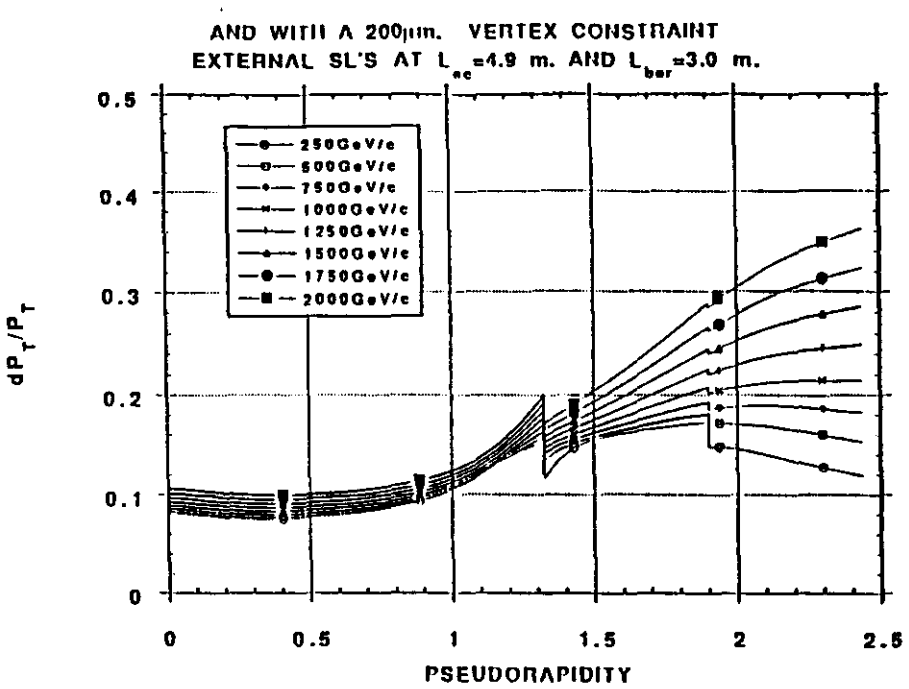
AND WITH A 200μm. VERTEX CONSTRAINT
EXTERNAL SL'S AT L_{ec}=4.9 m. AND L_{bar}=3.0 m.
250GeV/c
500GeV/c
750GeV/c
1000GeV/c
1250GeV/c
1500GeV/c
1750GeV/c
2000GeV/c
dP_T/P_T
PSEUDORAPIDITY

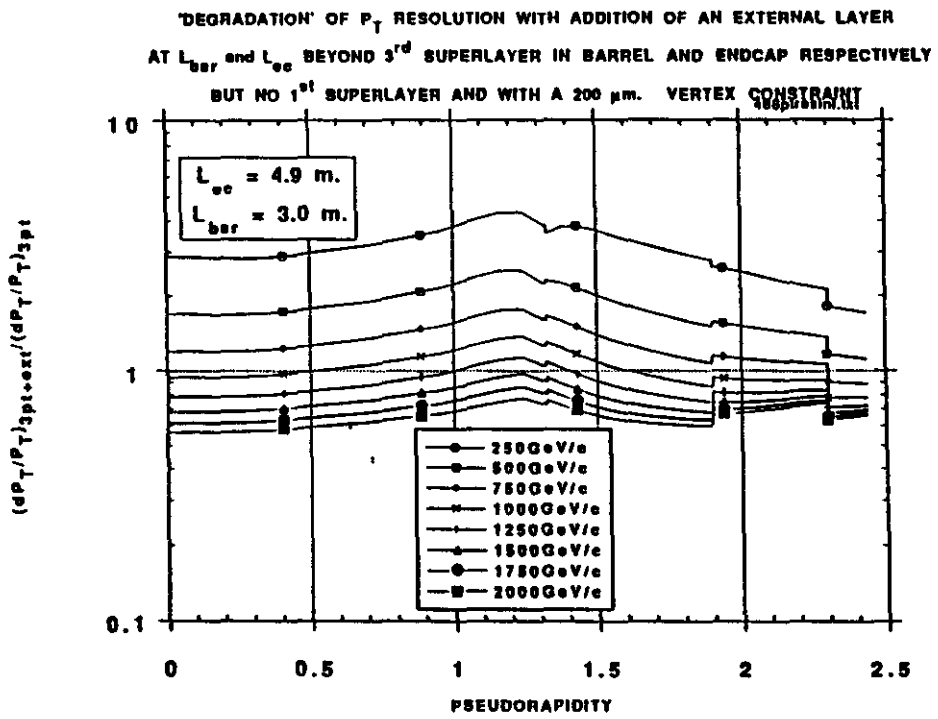
'DEGRADATION' OF P_T RESOLUTION WITH ADDITION OF AN EXTERNAL LAYER
AT L_{bar} and L_{ec} BEYOND 3rd SUPERLAYER IN BARREL AND ENDCAP RESPECTIVELY
BUT NO 1st SUPERLAYER AND WITH A 200 μm. VERTEX CONSTRAINT
L_{ec} = 4.9 m.
L_{bar} = 3.0 m.
250GeV/c
500GeV/c
750GeV/c
1000GeV/c
1250GeV/c
1500GeV/c
1750GeV/c
2000GeV/c
$(dP_T/P_T)_{3pt+ext}/(dP_T/P_T)_{3pt}$
PSEUDORAPIDITY

Fig. 10

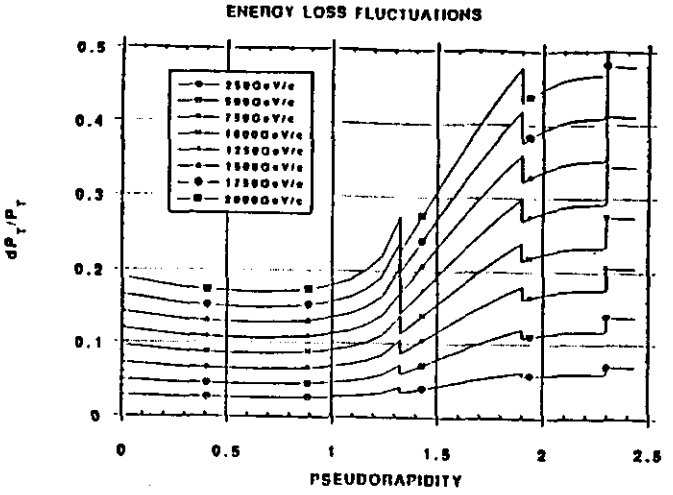
ENERGY LOSS FLUCTUATIONS
dP_T/P_T
PSEUDORAPIDITY

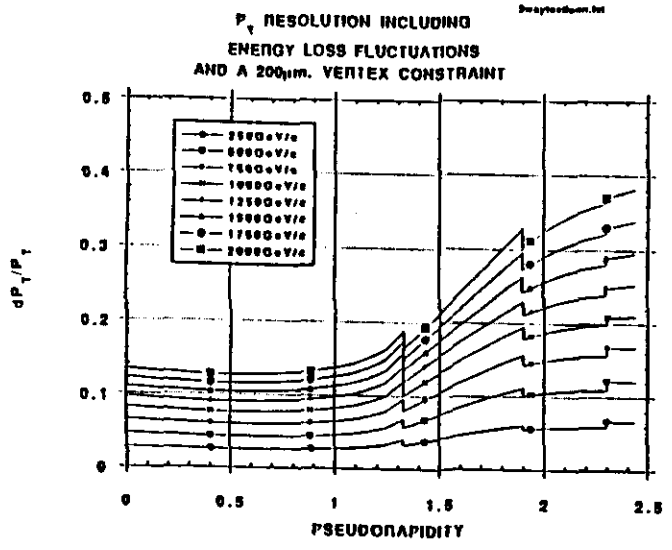
P_T RESOLUTION INCLUDING
ENERGY LOSS FLUCTUATIONS
AND A 200μm. VERTEX CONSTRAINT
dP_T/P_T
PSEUDORAPIDITY

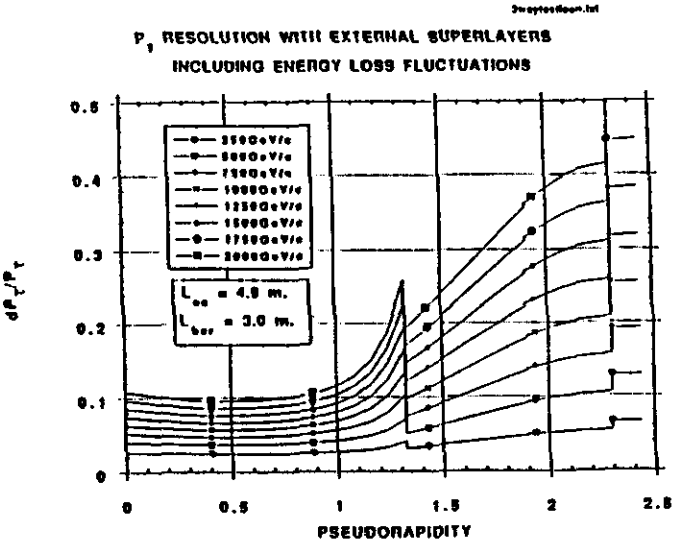
P_T RESOLUTION WITH EXTERNAL SUPERLAYERS
INCLUDING ENERGY LOSS FLUCTUATIONS
L_ee = 4.9 m.
L_bar = 3.0 m.
dP_T/P_T
PSEUDORAPIDITY

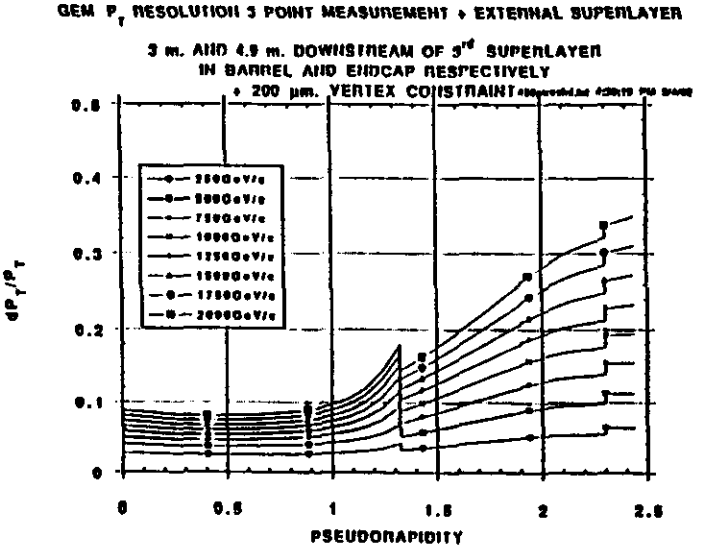
GEM P_T RESOLUTION 3 POINT MEASUREMENT + EXTERNAL SUPERLAYER
3 m. AND 4.9 m. DOWNSTREAM OF 3rd SUPERLAYER
IN BARREL AND ENDCAP RESPECTIVELY
+ 200 μm. VERTEX CONSTRAINT
dP_T/P_T
PSEUDORAPIDITY

Fig. 11

APPENDIX

IMPROVEMENT OF MOMENTUM RESOLUTION USING MEASUREMENTS OUTSIDE THE MAGNET

LARRY ROSENSON - MIT --7/11/91

ABSTRACT

The consideration of a magnet geometry with no return iron over most of the barrel region opens the possibility of significantly improving the momentum resolution of the system at high momenta (i.e. P > 500 GeV/c) by the addition of an additional Superlayer of detectors outside of the magnet coil. It is conjectured that this will be a cost effective design approach and it is proposed that such a feature be incorporated into the engineering design studies for the magnet and muon system.

It has been decided to pursue design studies on a magnet with a superconducting coil and with no return iron in the search for economies in the design of the detector. This approach immediately suggests the possible exploitation of the more open configuration by the extension of the muon system to include measurements outside the coil. Such measurements promise improved momentum resolution due to the effectively larger sagitta that will be measured if the effective point measurement errors can be kept approximately the same as for a measurement system all contained within the field. In addition, the use of a superconducting coil will tend to keep multiple scattering effects small. It is the purpose of this note to point out that such an approach is indeed feasible and in fact, that the potential gains are large enough to justify further investigation of such configurations.

In Fig. 1 we show a schematic drawing of the muon detection system.

We initially consider a detection system composed of the first three Superlayers, among which 16 layers of detecting planes with point resolution $\sigma_0 = 150$ μm. are distributed. All three Superlayers are assumed to lie inside the magnet so only the chamber material itself will give rise to relevant multiple scattering along the track. If Superlayer #1 and Superlayer #3 are separated by L the optimal position of Superlayer #2 is at L' = L/2. We call this arrangement the 'Sagitta' configuration. The optimal distribution of the 16 planes between the three Superlayers is then $N_1 = 4$, $N_2 = 8$ and $N_3 = 4$, where N_1, N_2 and N_3 are the number of planes in Superlayers #1, #2 and #3 respectively. We assume that the chamber planes are made of material with 0.025 radiation lengths per plane, giving 0.2 radiation lengths in Superlayer

#2. The uncertainty in momentum arising from imperfect alignment is taken into account by adding in quadrature to the ith Superlayer point resolution , $\sigma_0/\sqrt{N_i}$, a term, σ_{ext} , to account for the distribution in residual misalignment between the Superlayers, and a term, $\sigma_{int}/\sqrt{N_i}$, to account for the residual misalignment of planes with respect to each other within a Superlayer . We take $\sigma_0 = 150\mu m.$, $\sigma_{ext} = 25\mu m.$ and $\sigma_{int} = 50\mu m.$ in this example. The magnetic field B is taken equal to 1.0 tesla and the measuring interval L=5 m. The momentum resolution is shown in curve a) of Figure 2 .

As a second example we consider a three layer measurement provided by the same 16 planes but now placing the third Superlayer at D = 2 m outside the magnet coil. The coil is assumed to present 4 radiation lengths to the muon track. Superlayer #2 is moved downstream from it's previous location at L' = 2.5 m to L' = 3.2 m (this would be the the optimal position if there were no multiple scattering in the coil and detectors) Again we distribute the 16 planes optimally (within roundoff) resulting in $N_1 = 4$, $N_2 = 8$ and $N_3 = 4$. We call this arrangement the 'Outside Lever Arm' configuration. The momentum resolution is shown in curve b) of Figure 2.

From Figure 2 we see that the Sagitta measurement is better at momenta well below 250 GeV/c and the Outside Lever Arm measurement is better at momenta well above 250 GeV/c. This behavior is qualitatively true for any range of values of the radiation thickness' of the coil and detector planes likely to arise in practice. The difference in performance is significant in both momentum regions and if a choice had to be made between the two approches it would have to be made on the basis of Physics priorities and prognostications which are very difficult to make at this time.

A simple redeployment of the 16 layers can give us the best features of both measurement strategies. We retain three Superlayers inside the field in the geometry of the 'Sagitta' measurement and with a sufficient number of planes to provide almost the optimal Sagitta measurement and we add a fourth layer to the system at D = 2m. outside the coil. We take as an example $N_1 = 4$, $N_2 = 7$ and $N_3 = 3$ and $N_4 = 2$. We show the resulting momentum resolution as curve c) in Figure 3. Curves a) and b) from Figure 2 are shown for reference. It is clear that with this 'Four Point Measurement' configuration we essentially completely recover the low momentum Sagitta measurement and almost completely recover the high momentum Outside Lever Arm behavior.

In Figure 4 we show the dependence of the Four Point Measurement on the radiation thickness of the coil over the range $2 \leq n_{coil} \leq 10$, where

n_{coil} is the number of radiation lengths in the coil. The relative insensitivity of the basic result to the coil thickness is an important aspect of the robustness of the Four Point Measurement as a design concept.

As is well known, the most important sensitivity of the detector system is to the quality of the alignment of the system. In particular the main effect is due to relative misalignment of the Superlayers which we have parameterized with σ_{ext}. In Figure 5 we show the variation of the Four Point Measurement momentum resolution to σ_{ext} over the range $0 \leq \sigma_{ext} \leq 100$ μm. All the other parameters have the same values as in curve c) in Figure 3. Significant degradation of the resolution occurs for $\sigma_{ext} \geq 50$ μm. A comparable sensitivity occurs also for the Sagitta strategy and is shown in Figure 6.

It is fair to ask whether one will be able to achieve the same quality of alignment for the proposed Fourth Superlayer which lies outside the magnet coil and can only with some difficulty be physically or even optically coupled to the inner three Superlayers. In Figure 7 we show the sensitivity of the resolution to variation in $\sigma_{ext\text{-}Superlayer\ \#4}$, the alignment uncertainty of the fourth Superlayer, for the range 25 μm.$\leq \sigma_{ext\text{-}Superlayer\ \#4} \leq 200$ μm. All other parameters are the same as in curve c) of Figure 3. From Figure 7 we see that as long as $\sigma_{ext\text{-}Superlayer\ \#4} \leq 100$ μm. we will not degrade the momentum resolution catastrophically.

In conclusion it appears that a significant improvement in the momentum resolution at high momenta(a factor of about 0.7) can be obtained over that achievable with a Sagitta measurement by redeploying several detector planes to the outside of the magnet. The alignment requirement of such a Superlayer must be carefully studied to see whether it presents any insuperable problems. The possible gain in resolution would seem to be large enough to strongly suggest the inclusion of this approach in the cost effectiveness optimization of the magnet/muon system.

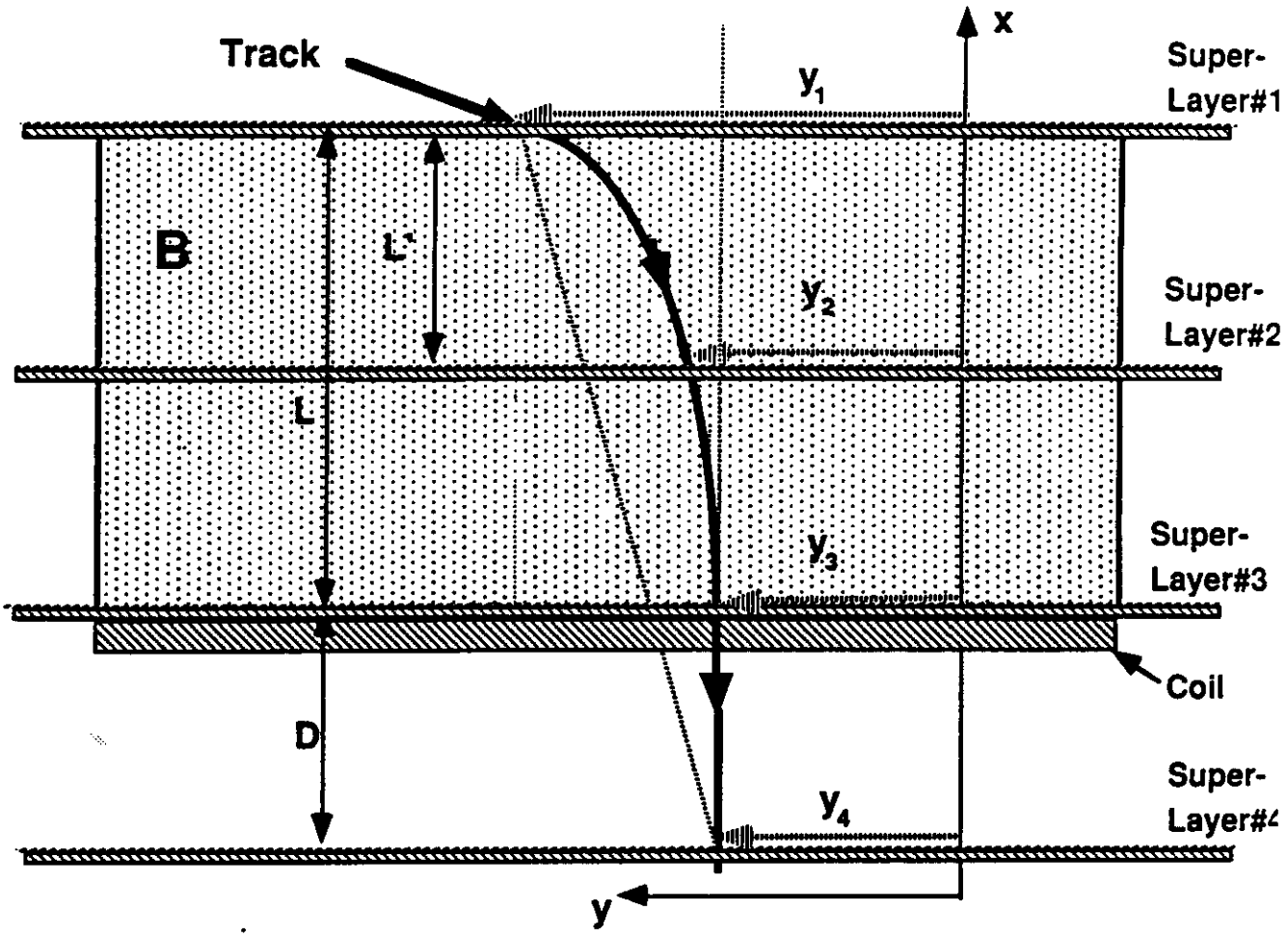

Figure 1
Schematic of the muon detection system.

In a region with uniform magnetic field, B, the track first crosses detector Superlayer #1. It then crosses Superlayer #2 at L' and Superlayer #3 at L, at which point it passes through the coil and leaves the magnetic field. An optional fourth Superlayer is located a distance D outside the coil. Measurements are made of the y_i by suitably averaging point measurements in the measurements made in the N_i planes in the ith Superlayer. The 'Sagitta' measurement may be thought of as utilizing only Superlayers #1, #2 and #3. The 'Outside Lever Arm' measurement may be thought of as utilizing only Superlayers #1, #2 and #4. The 'Four Layer ' measurement uses all four Superlayers as drawn.

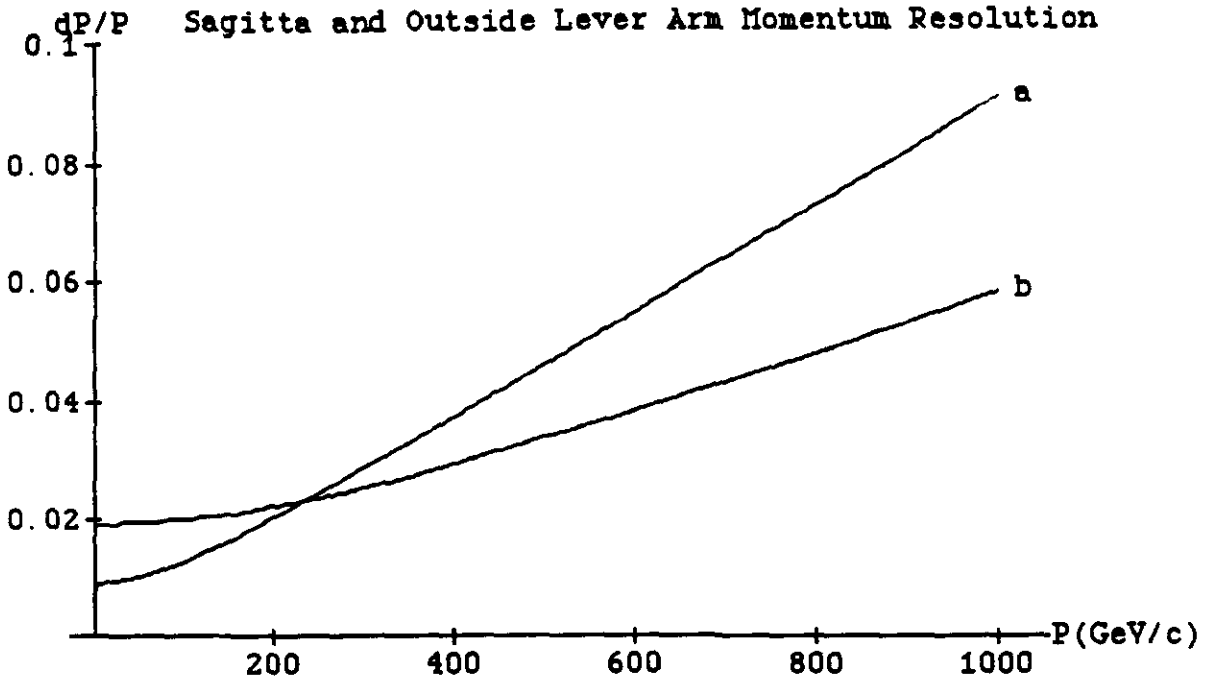

Figure 2

Momentum resolution for the Sagitta and Outside Lever Arm strategies. Curve a - Sagitta Measurement; Curve b- Outside Lever Arm. Measurement

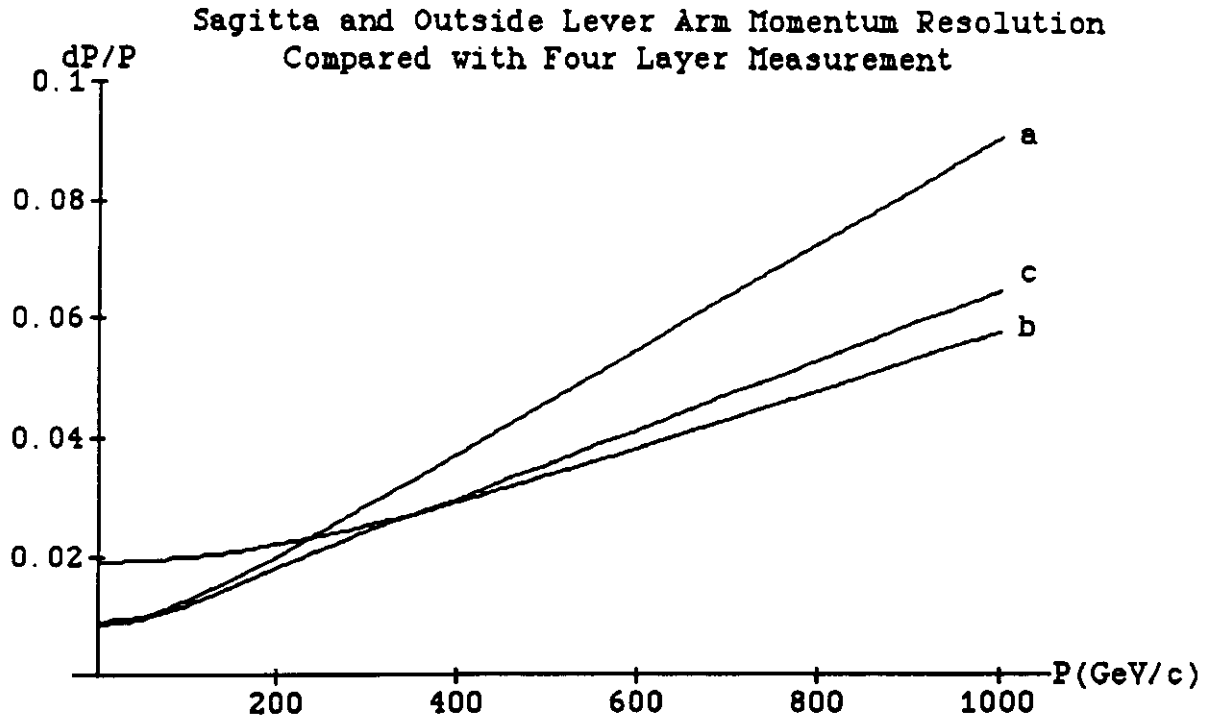

Figure 3

Comparison of Four Layer Measurement Momentum resolution with that of the Sagitta and Outside Lever Arm strategies. Curve a - Sagitta Measurement; Curve b- Outside Lever Arm.Measurement;Curve c) - Four Layer Measurement.

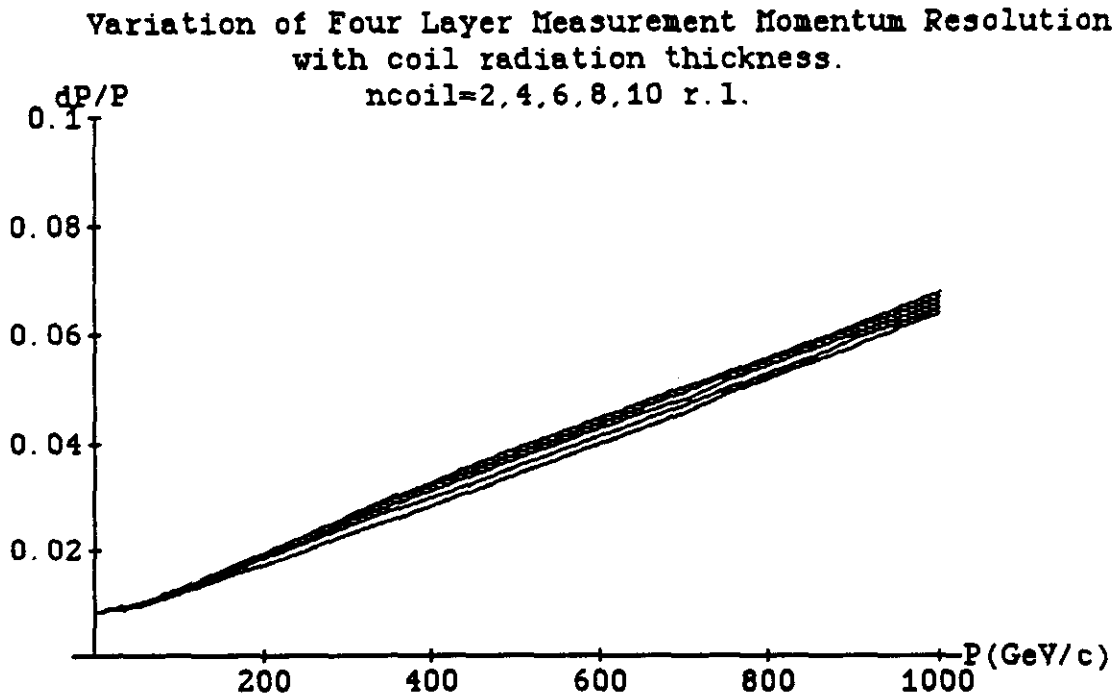

Figure 4

Variation of Four Layer Measurement Momentum Resolution with coil radiation thickness ,n_{coil} . The lowest curve corresponds to $n_{coil} = 2$ radiation lengths. The curves successively correspond to increments of $n_{coil} = 2$ radiation lengths.

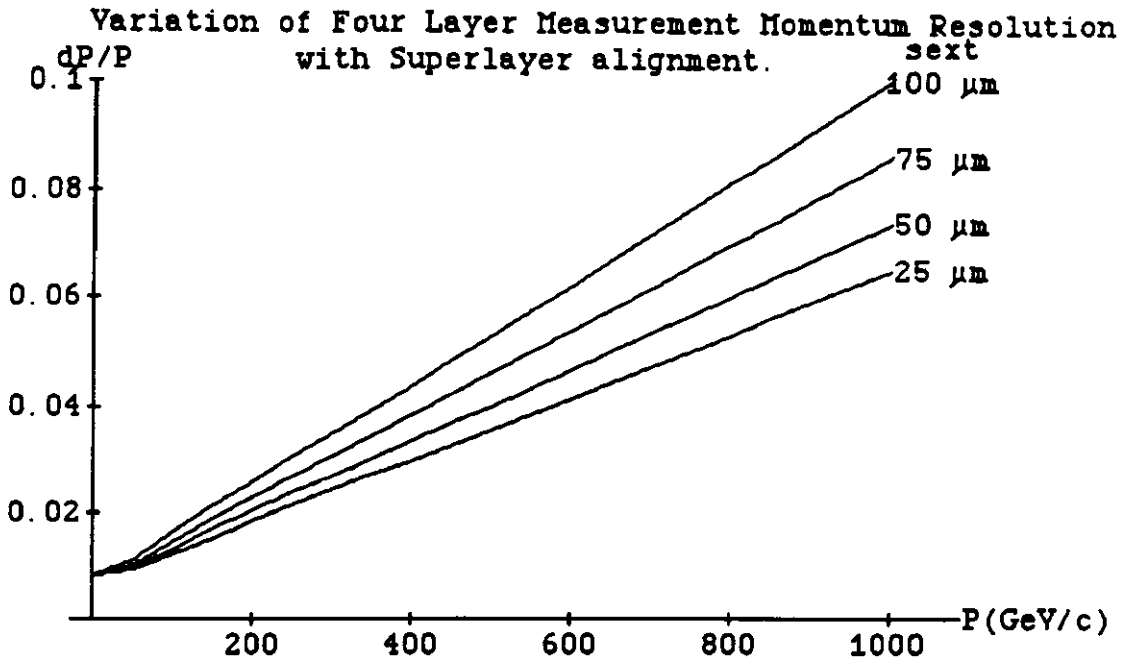

Figure 5

Variation of Four Layer Measurement Momentum Resolution with Superlayer Alignment. The nominal configuration is the lowest curve corresponding to $\sigma_{ext} = 25\mu m$. The successively increasing curves correspond to $\sigma_{ext} = 50\mu m.$, $\sigma_{ext} = 75\mu m.$and $\sigma_{ext} = 100\mu m$.

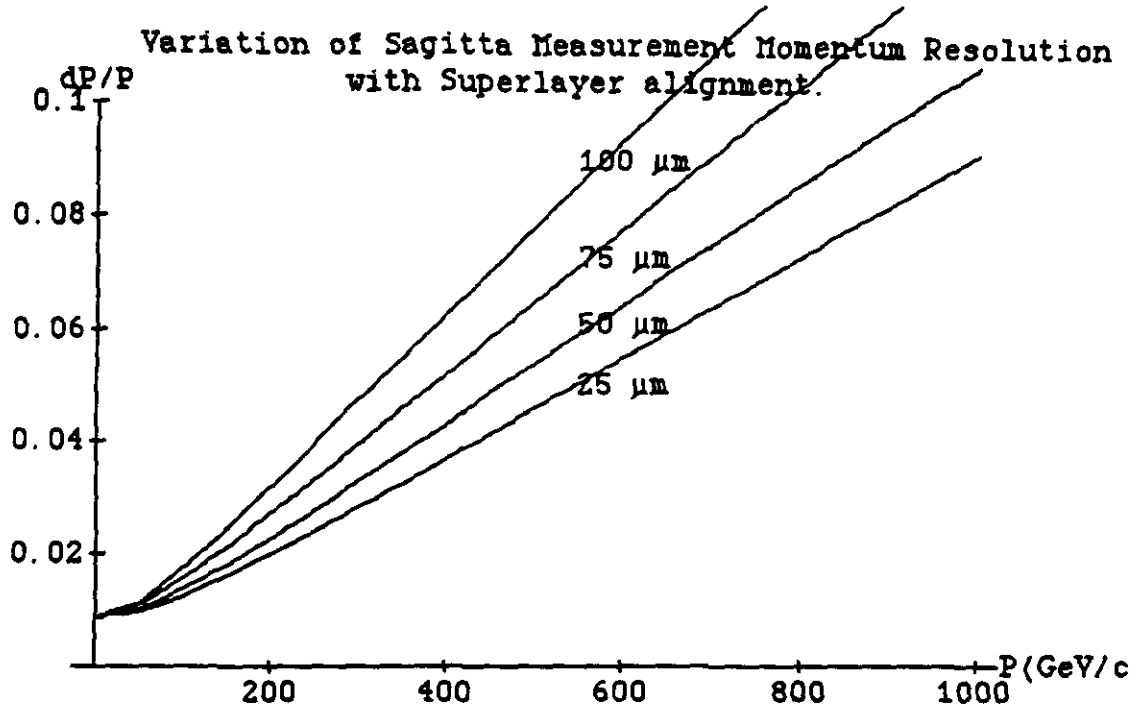

Figure 6

Variation of Sagitta Measurement Momentum Resolution with Superlayer Alignment. The nominal configuration is the lowest curve corresponding to σ_{ext} = 25µm. The successively increasing curves correspond to σ_{ext} = 50µm., σ_{ext} = 75µm.and σ_{ext} = 100µm.

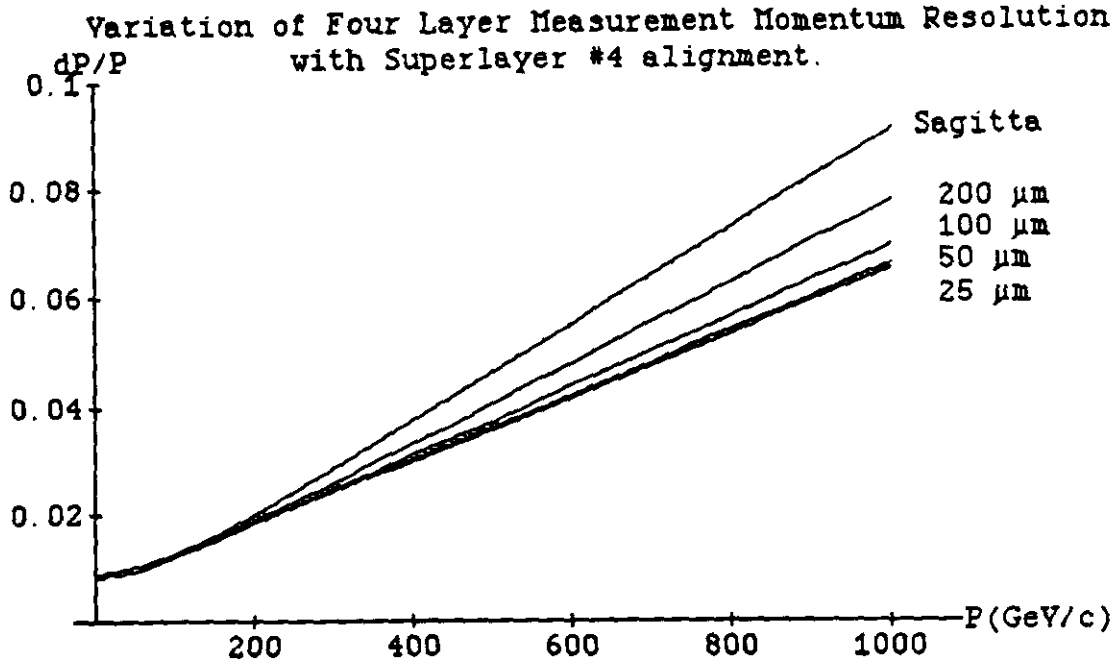

Figure 7

Variation of Four Layer Measurement Momentum Resolution with Superlayer #4 Alignment. The four lowest curves correspond to $\sigma_{ext\text{-}Superlayer\ \#4}$ ranging from 25 µm. to 200 µm. The highest curve, labeled 'Sagitta', is a reproduction of Figure 2 curve a) for comparison. It is close to the limiting resolution from the Four Point Measurement for a completely useless coordinate measurement by Superlayer.#4 and gives a scale for the degradation arising from misalignment of this Superlayer.